

Development of nickel and magnetite promoted carbonized cellulose beads supported bimetallic Pd-Pt catalysts for hydrogenation of chlorate ions in aqueous solution

Emőke Sikora<sup>1,2,a</sup>, Dániel Koncz-Horváth<sup>2,b</sup>, Gábor Muránszky<sup>1,2,c</sup>, Ferenc Kristály<sup>3,d</sup>,  
Béla Fiser<sup>1,2,4,e</sup>, Béla Viskolcz<sup>1,f</sup>, László Vanyorek<sup>1,g\*</sup>

<sup>1</sup>Institute of Chemistry, University of Miskolc, 3515 Miskolc-Egyetemváros, Hungary

<sup>2</sup>Higher Education Industry Cooperation Centre, University of Miskolc, 3515 Miskolc-Egyetemváros, Hungary

<sup>3</sup>Institute of Mineralogy and Geology, University of Miskolc, 3515 Miskolc-Egyetemváros, Hungary

<sup>4</sup>Ferenc Rákóczi II. Transcarpathian Hungarian College of Higher Education, 90200 Beregszász, Transcarpathia, Ukraine

\* Corresponding author

<sup>a</sup>kemsik@uni-miskolc.hu, <sup>b</sup>femkhd@uni-miskolc.hu, <sup>c</sup>kemmug@uni-miskolc.hu, <sup>d</sup>askkf@uni-miskolc.hu,  
<sup>e</sup>kemfiser@uni-miskolc.hu, <sup>f</sup>bel.viskolcz@uni-miskolc.hu, <sup>g</sup>kemvanyi@uni-miskolc.hu

SUPPLEMENTARY INFORMATION

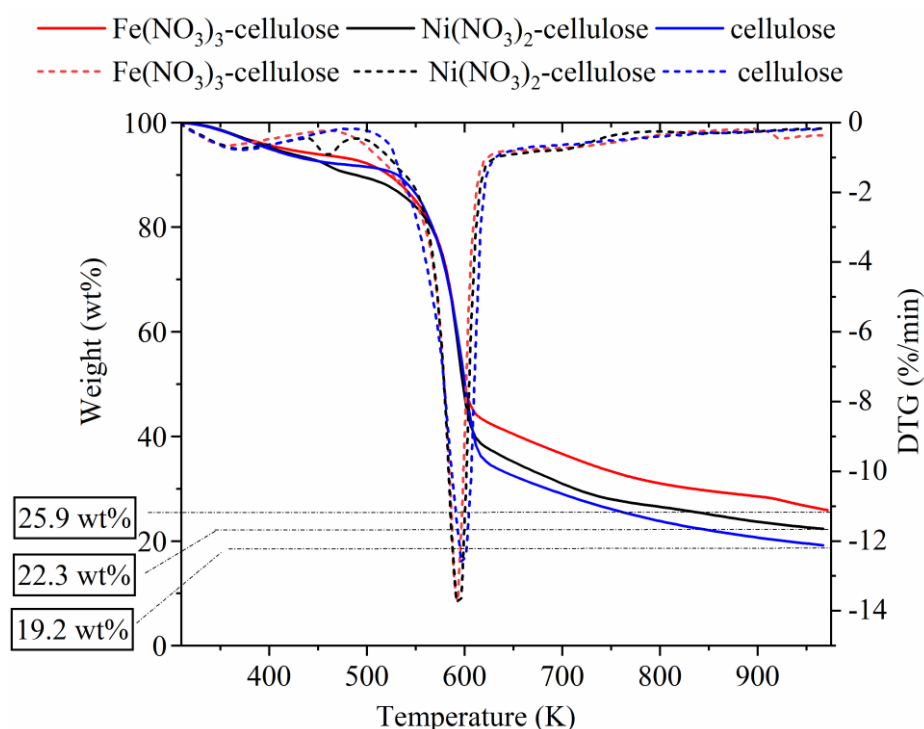


Figure S1. TG-DTG curves of the impregnated (with iron(III) nitrate or nickel(II) nitrate) cellulose beads (CB) and the non-impregnated sample.

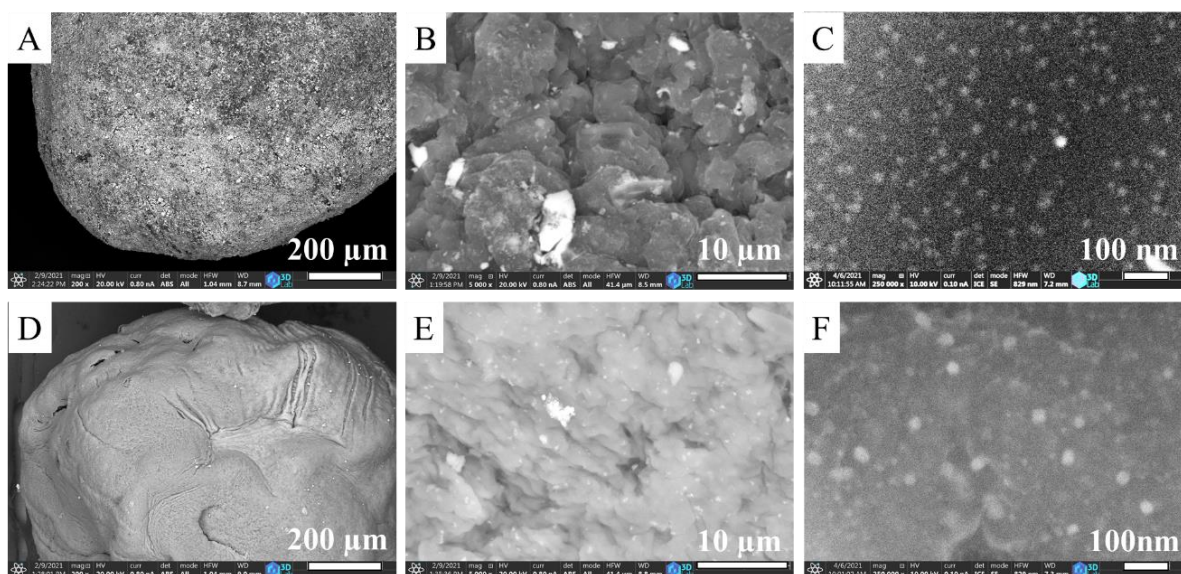


Figure S2. SEM images of the surface morphology of the  $\text{Fe}_3\text{O}_4\text{-CCB}$  (A-C), and  $\text{Ni-CCB}$  (D-F) catalyst supports.

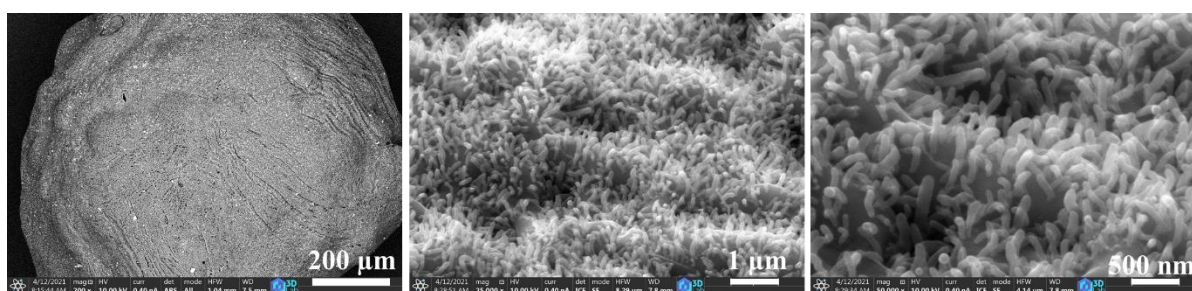


Figure S3. SEM images of the surface morphology of the non-impregnated carbonized cellulose bead (CCB) catalyst support.

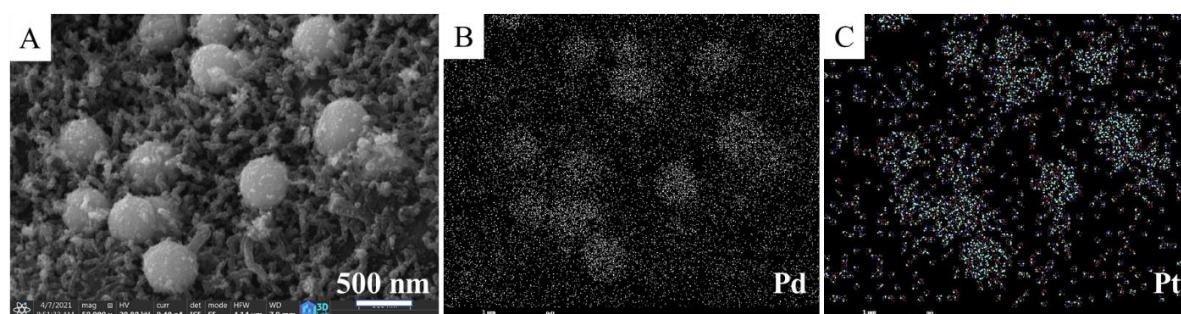


Figure S4. Elemental maps of the aggregated particles on the surface of the  $\text{Pd-Pt/CCB}$  catalyst with the localization of palladium (B) and platinum (C).

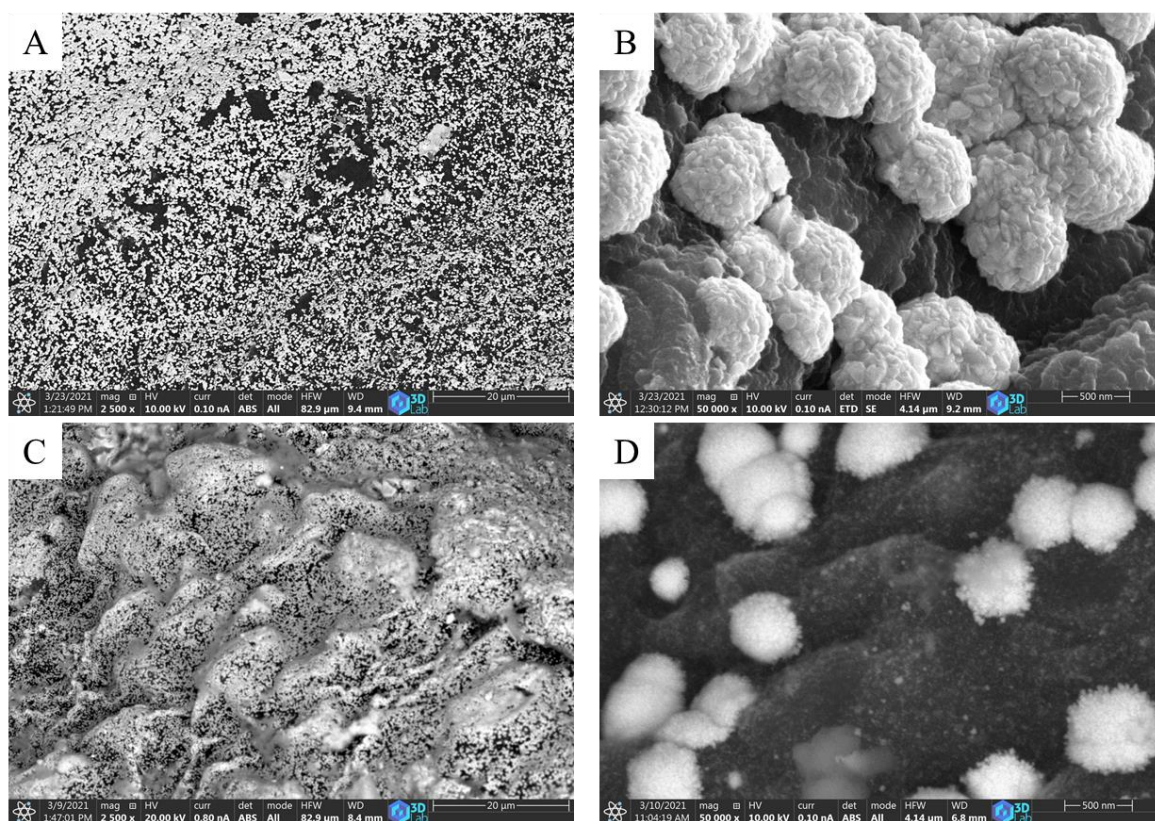


Figure S5. SEM images of the palladium and platinum nanoparticle based aggregated crystallites on the surface of the Fe<sub>3</sub>O<sub>4</sub>-CCB (A, B) and Ni-CCB (C, D) catalyst supports shown at different magnifications.



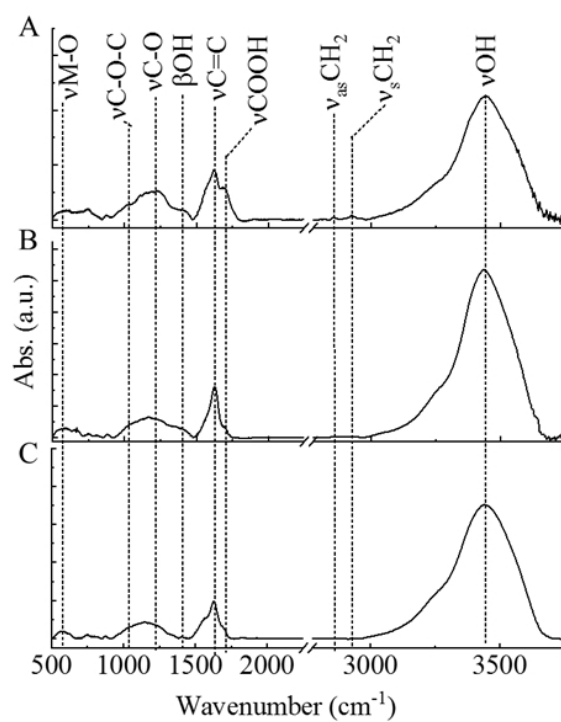


Figure S6. FTIR spectra of the 5 times used Pd-Pt/CCB (A), the Pd-Pt/Ni-CCB (B), Pd-Pt/Fe<sub>3</sub>O<sub>4</sub>-CCB (C) catalysts.

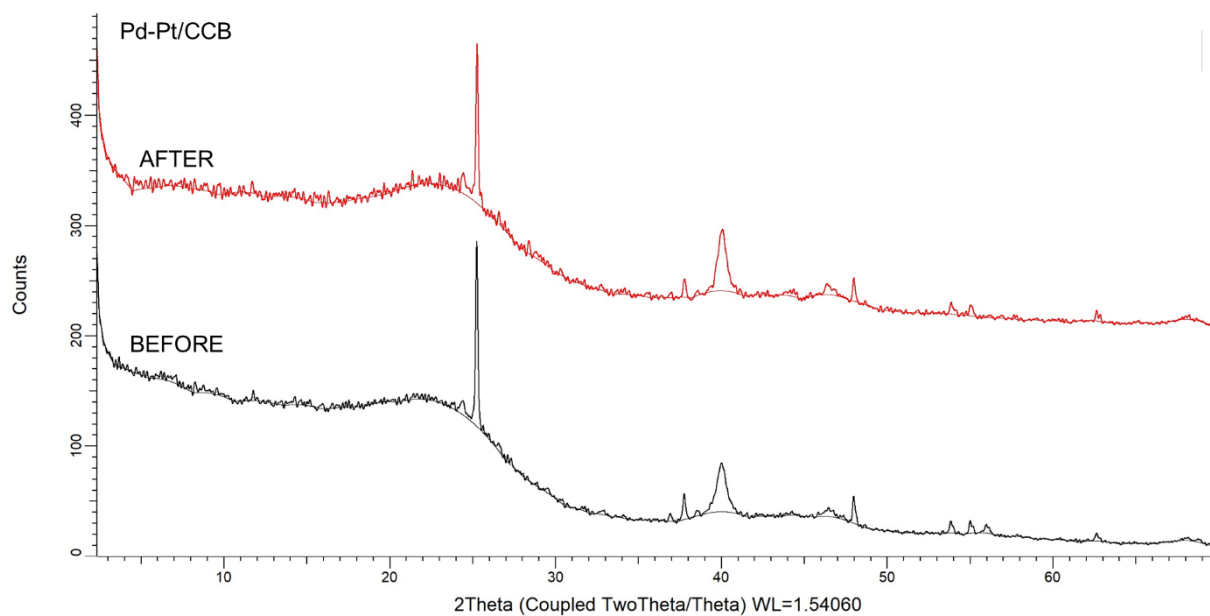


Figure S7. XRD patterns of the fresh (before) and the 5 times used (after) Pd-Pt/CCB catalyst.

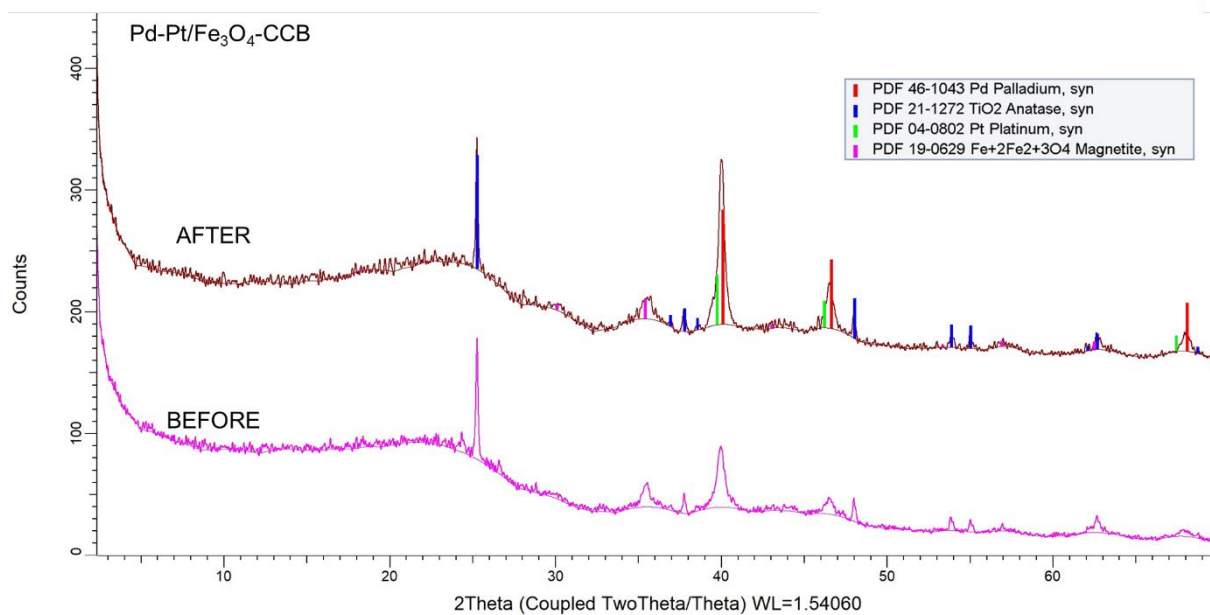


Figure S8. XRD patterns of the fresh (before) and the 5 times used (after) Pd-Pt/Fe<sub>3</sub>O<sub>4</sub>-CCB catalyst.

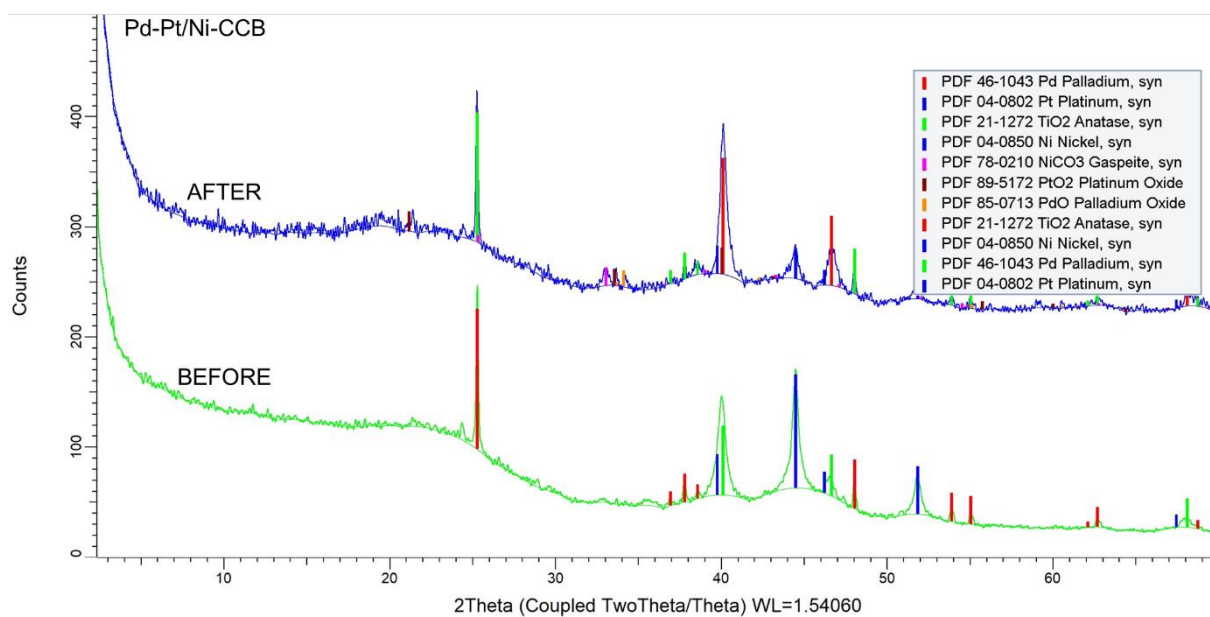


Figure S9. XRD patterns of the fresh (before) and the 5 times used (after) Pd-Pt/Ni-CCB catalyst.

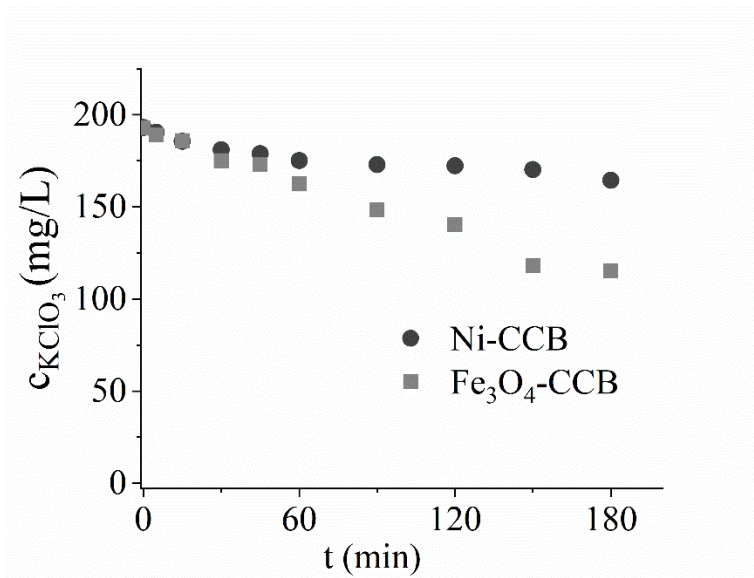


Figure S10. Chlorate conversion *vs.* time of hydrogenation. Catalytic activity of the Ni-CCB and Fe<sub>3</sub>O<sub>4</sub>-CCB supports.

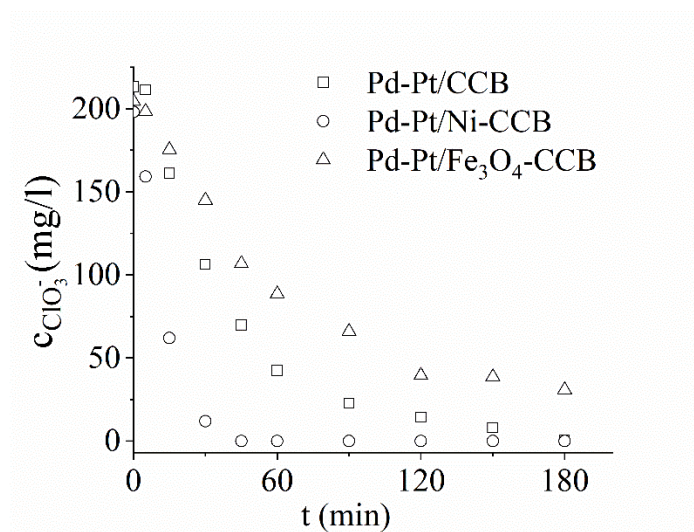


Figure S11. Chlorate conversion *vs.* time of hydrogenation by using the developed Pd-Pt/CCB, Pd-Pt/Ni-CCB, and Pd-Pt/Fe<sub>3</sub>O<sub>4</sub>-CCB catalysts.

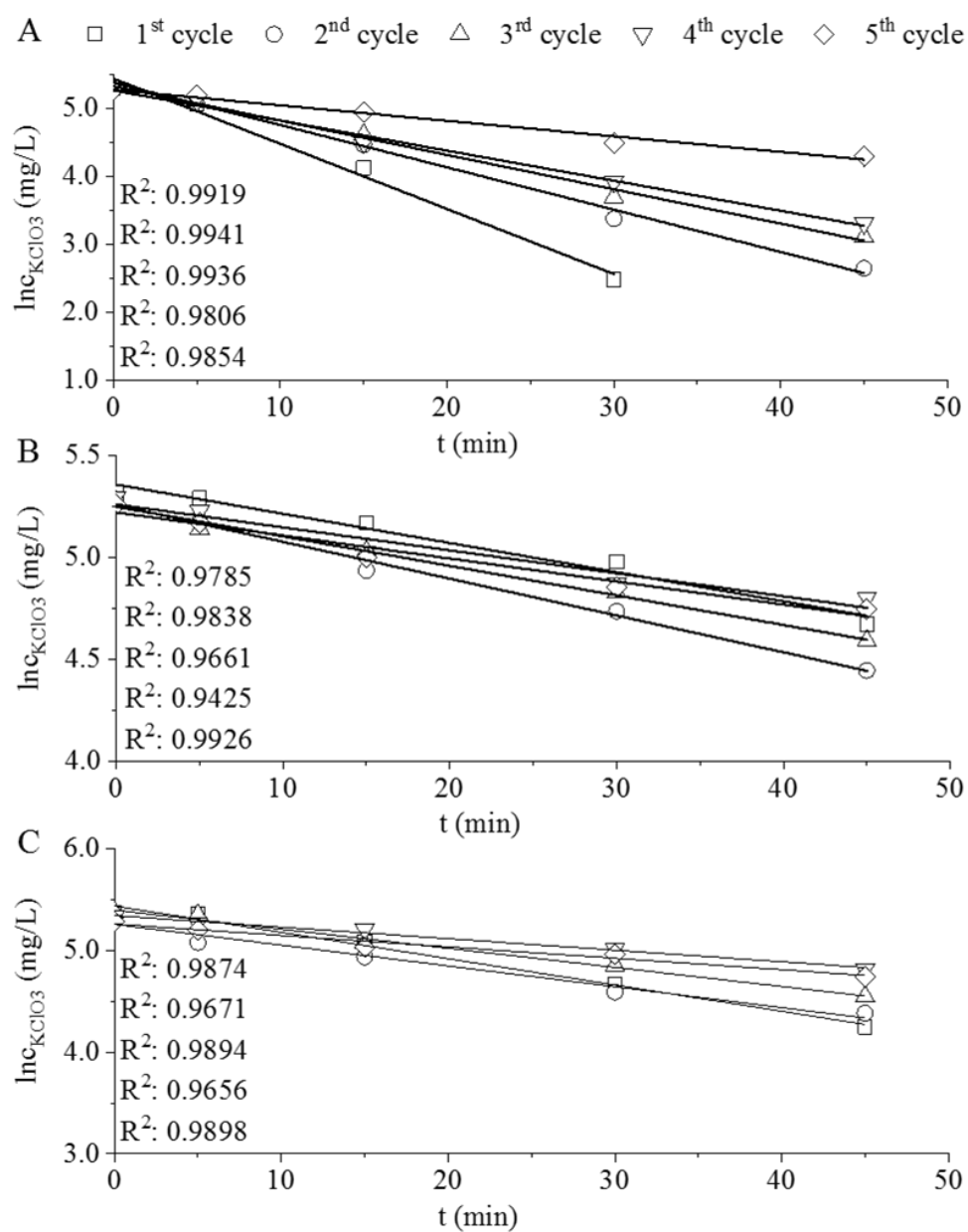


Figure S12.  $\text{Inc}$  vs. time (min) after the reuse tests by using the Pd-Pt/Ni-CCB (A), Pd-Pt/Fe<sub>3</sub>O<sub>4</sub>-CCB (B), and Pd-Pt/CCB (D) catalysts.

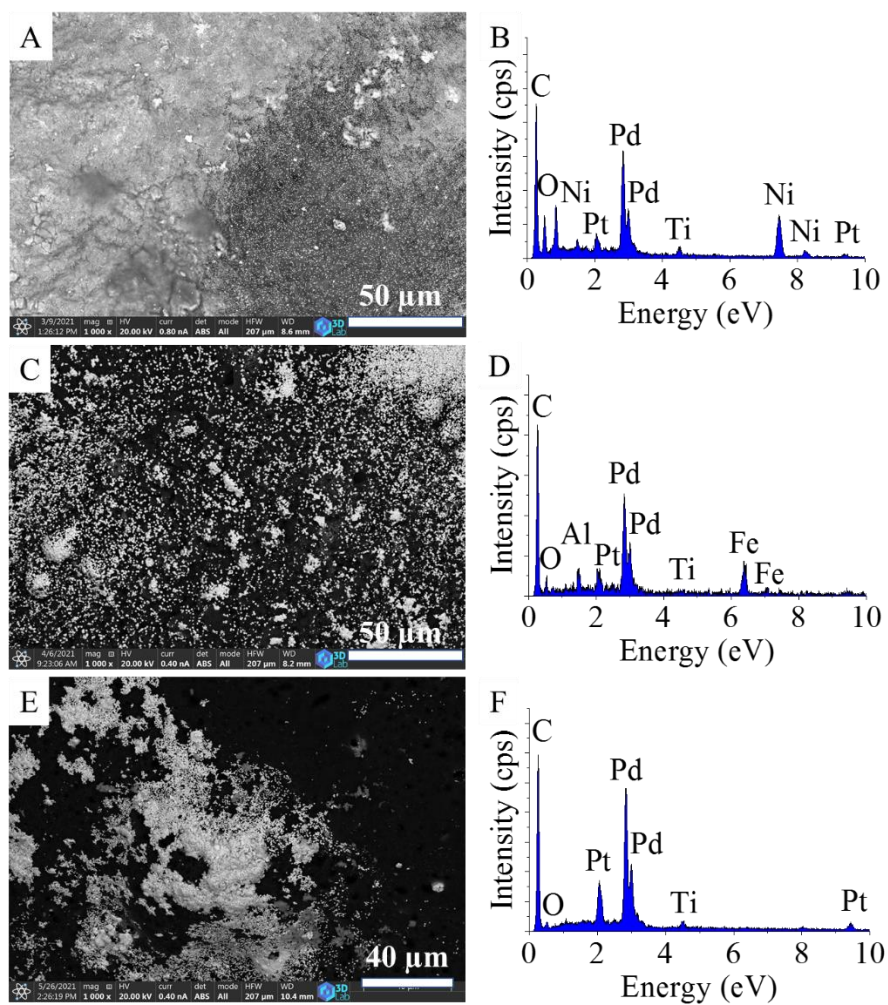


Figure S13. SEM images and EDS spectra of the Pd-Pt/Fe<sub>3</sub>O<sub>4</sub>-CCB (A, B), Pd-Pt/Ni-CCB (C, D), and Pd-Pt/CCB (E, F) catalyst after five reuse cycles.